Electronic Supplementary Material (ESI) for Inorganic Chemistry Frontiers.

Multi-shelled $LiMn_2O_4$ hollow microspheres as superior cathode materials for Lithium-ion batteries

Feng Wang,‡[a] Jiangyan Wang,‡[b,d] Hao Ren,[a] Hongjie Tang,[b] Ranbo Yu,*[a] and Dan Wang*[b,c]

[a]Department of Physical Chemistry, School of Metallurgical and Ecological Engineering, University of Science and Technology Beijing, No. 30, Xueyuan Road, Haidian District, Beijing 100083, P. R. China, Email: ranboyu@ustb.edu.cn

[b]National Key Laboratory of Biochemical Engineering, Institute of Process Engineering, Chinese Academy of Sciences, No. 1 Beiertiao, Zhongguancun, Beijing 100190, P. R. China, Email: danwang@ipe.ac.cn

[c]Centre for Clean Environment and Energy, Gold Coast Campus Griffith University, Queensland 4222, Australia

[d]University of Chinese Academy of Sciences, No.19A Yuquan Road, Beijing 100049, P. R. China

Supporting information

Experimental section:

Synthesis of multi-shelled $LiMn_2O_4$ hollow spheres: All reagents were purchased from Beijing Chemical Co., Ltd., and of analytical grade, used without further purification. Lithium acetate (LiAc) and manganese nitrate tetrahydrate ($Mn(NO_3)_2$ $4H_2O$) were used as metal precursors. Typically, the synthesis process of triple-shelled $LiMn_2O_4$ hollow microspheres was described below as an example. The carbonaceous

microsphere templates were prepared through the emulsion polymerization reaction of sucrose under the hydrothermal conditions as described elsewhere.[S1] Freshly-prepared CMSs (0.6 g) were dispersed in 30ml lithium acetate and manganese nitrate solution (the concentration of Li salt and Mn salt was 1 M and 0.1 M, respectively) with the aid of ultrasonication. After ultrasonic dispersion for 10-20 min, the resulting suspension was further aged for 12 h at 30 ℃ in a water bath, then filtered with a vacuum pump and washed with DI water for three times, and then dried at 80 ℃ in an oven for 12-24 h. The resultant composite microspheres were heated to 600 ℃ in air at the rate of 1 ℃ min^{-1}, and kept at 600 ℃ for 2 h, then cooled down to room temperature naturally. The triple-shelled $LiMn_2O_4$ hollow microspheres were collected as black powders. The synthesis processes of quadruple-shelled $LiMn_2O_4$ hollow microspheres is very similar to which of the triple-shelled $LiMn_2O_4$ hollow microspheres, except the minor differences in aging duration and heating rate (experimental details can be seen in Table S2).

Materials characterization: Powder X-ray diffraction (XRD) patterns were carried out though the Panalytical X'Pert PRO MPD [Cu Ka radiation (λ = 1.5405 Å)], operating at 40 kV and 30 mA. Scanning electron microscopy (SEM) images were obtained using a JSM-6700 microscope operating at 5.0 kV. Transmission electron microscopy (TEM) images were taken on a FEI Tecnai F20 instrument using an accelerating voltage of 200 kV. The nitrogen adsorption-desorption isotherms under liquid nitrogen (-196 ℃) were measured on a Quantochrome Autosorb-1MP sorption analyzer with pre-degassing treatment under vacuum at 200 ℃ overnight. XPS data

were recorded through an ESCALab220i-XL electron spectrometer from VG Scientific using 300 W Al Kα radiation. The binding energies obtained in the XPS analysis were standardized according to C 1s (284.8 eV).

Electrochemical measurement: The electrochemical performance of the prepared $LiMn_2O_4$ products was carried out using CR2032 coin type cells with Li metal as the counter and reference electrodes at room temperature. The electrolyte was 1 M $LiPF_6$ in a mixture of ethylene carbonate and diethyl carbonate (50:50 w/w). The working electrode was fabricated by compressing a mixture of the active materials, conductive material (carbon black), and binder (polyvinylidene fluoride, PVDF) in a weight ratio of $LiMn_2O_4$/carbon/PVDF = 7:2:1 onto an aluminum foil current collector. The loading amount of active materials is about 1 mg/cm^2. The cells were assembled in an argon-filled glove box with the concentrations of moisture and oxygen at below 1 ppm. The electrode capacity was measured by a galvanostatic discharge-charge method between 3.5 and 4.3 V at rates of 1 C, 2 C, 4 C, 8 C or 10 C at a battery test system (Neware BST-5 V 5 mA). CV curves were tested between 3.5-4.3 V (vs. Li^+/Li) at a constant scan rate of 1 mV/s. Electrochemical impedance spectroscopy (EIS) tests were obtained over the frequency ranging from 1 to 10^5 Hz with an ac amplify voltage of 10 mV.

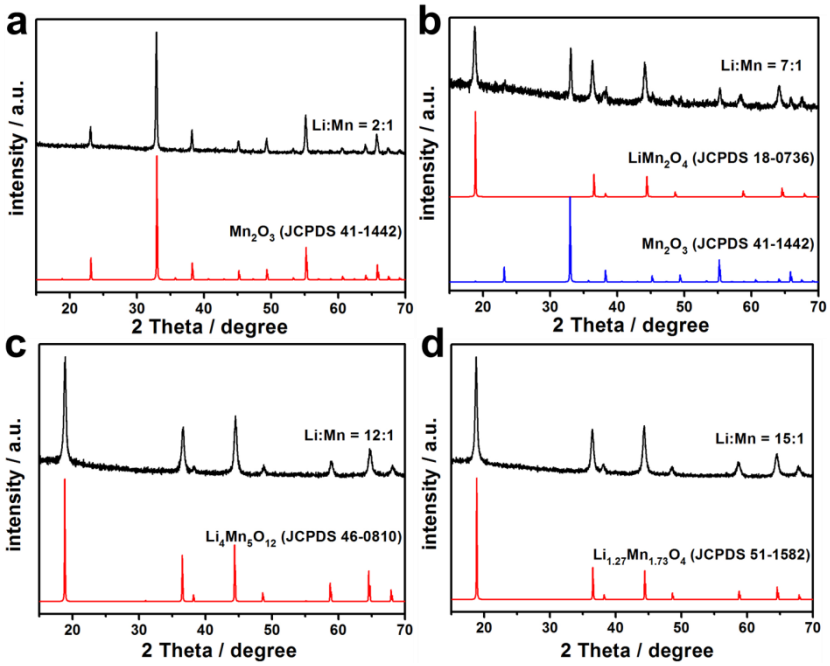

Figure S1 The effect of adding ratio of Li precursor to Mn precursor on the composition of the products.

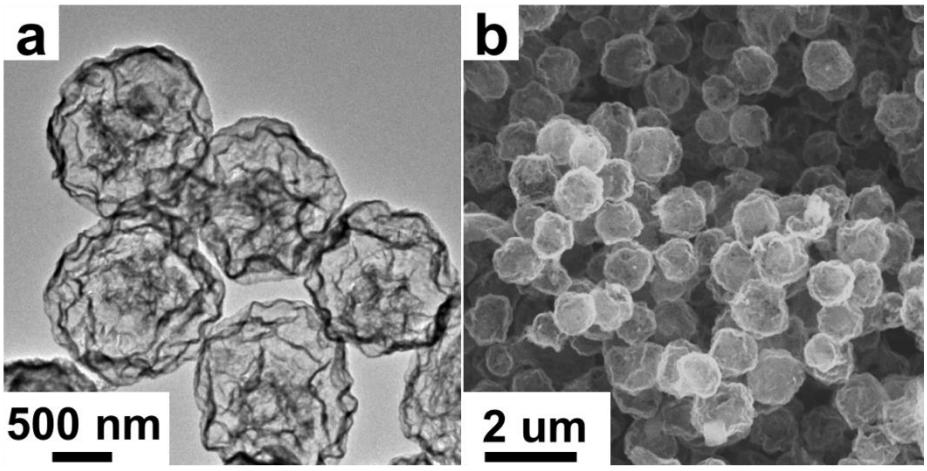

Figure S2 (a) TEM and (b) SEM images of double-shelled hollow microspheres gotten under a heating rate of 10 ℃/min.

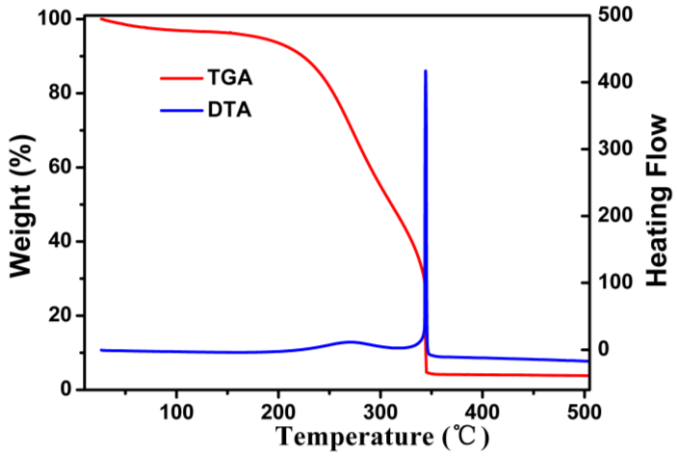

Figure S3 TGA and DTA curves of carbonaceous microspheres with Li and Mn ions infused under air atmosphere at a heating rate of 1 ℃ min^{-1}.

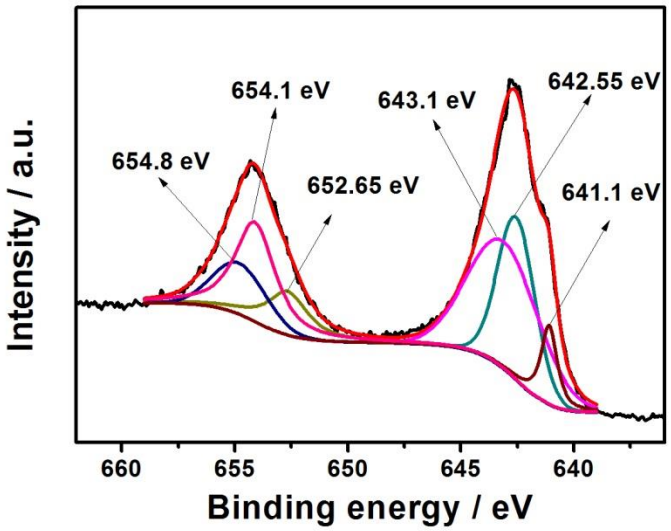

Figure S4 XPS spectra of Mn 2p of multi-shelled $LiMn_2O_4$ hollow microspheres.

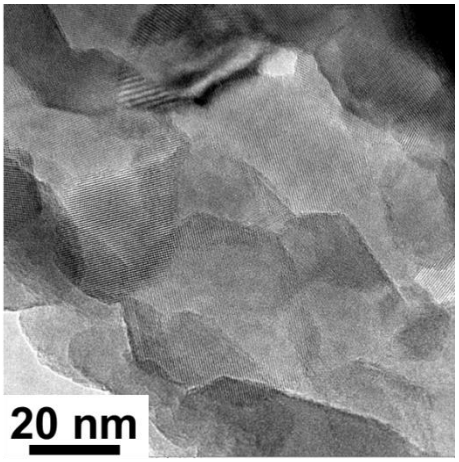

Figure S5 Enlarged TEM images of the shell on the 3S-$LiMn_2O_4$-HMSs.

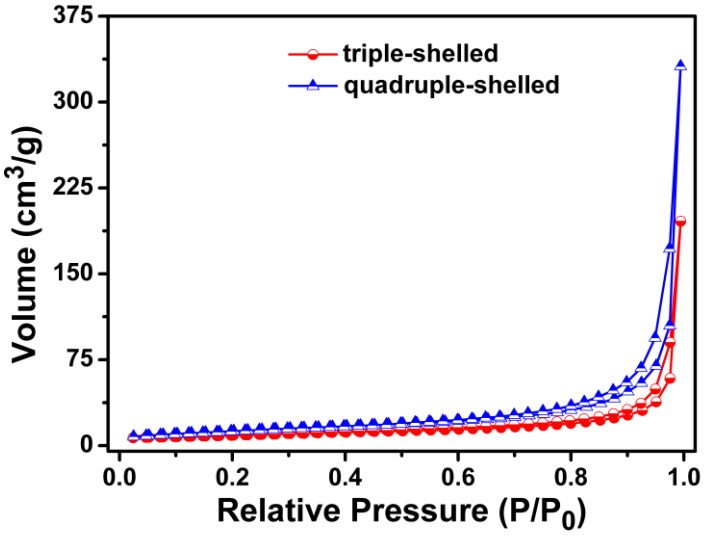

Figure S6 Nitrogen adsorption–desorption isotherm of multi-shelled $LiMn_2O_4$ hollow microspheres.

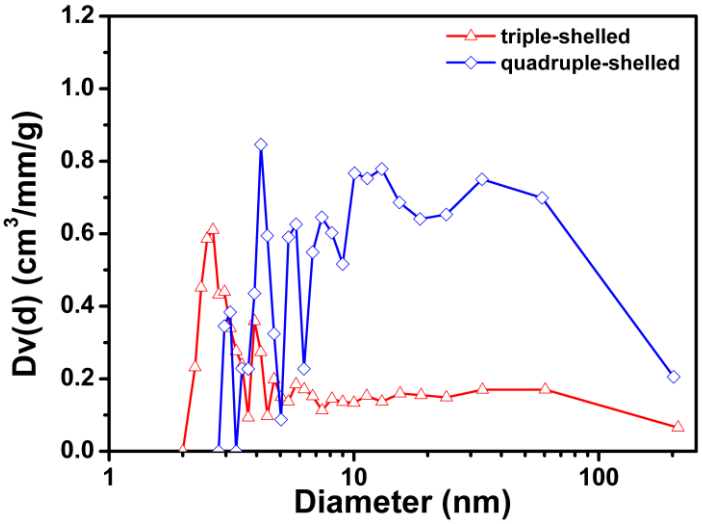

Figure S7 Barret-Joyner-Halenda (BJH) pore-size distribution curves of multi-shelled $LiMn_2O_4$ hollow microspheres according to the nitrogen adsorption–desorption isotherm.

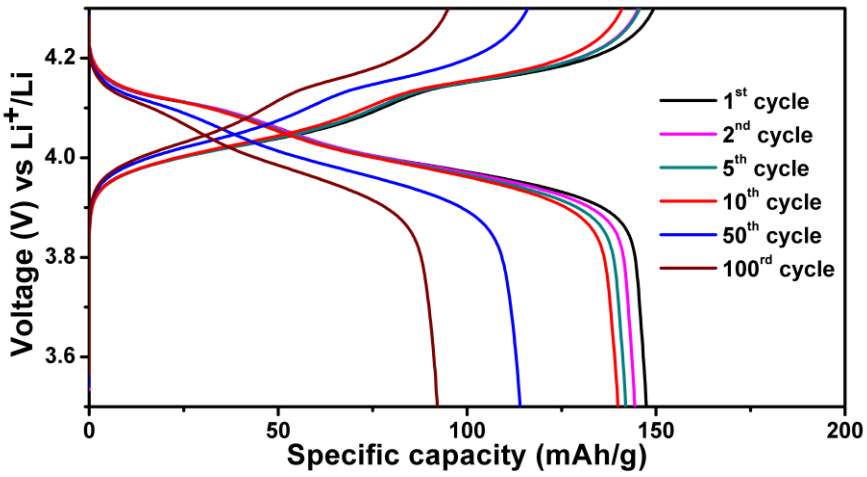

Figure S8 Discharge-charge curves of the quadruple-shelled hollow microspheres at different cycle numbers with a constant rate of 1 C (assuming 1 C = 148 mA/g).

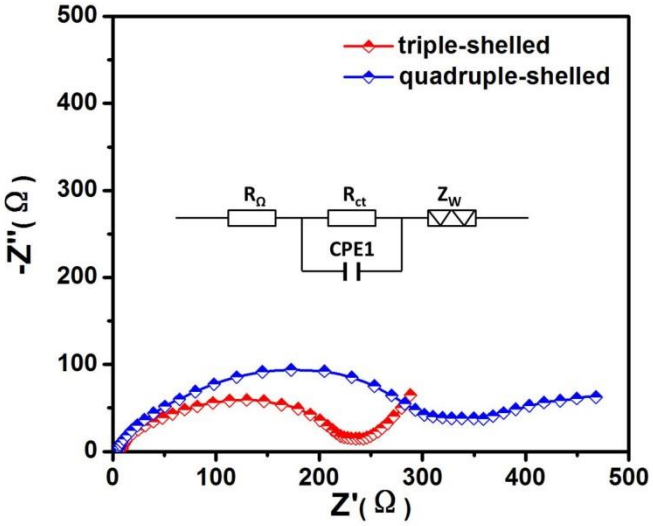

Figure S9 Electrochemical impedance spectra (EIS) for multi-shelled $LiMn_2O_4$ hollow microspheres after 100 cycles with the simplified Randles equivalent circuit model inset (RΩ, external resistance; Rct, charge transfer resistance; CPE1, constant phase element; Zw, Warburg impedance).

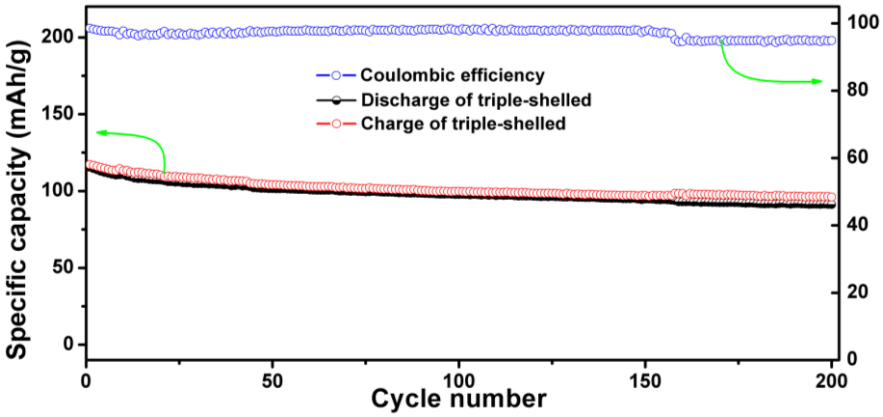

Figure S10 Long-term cycling performance and Coulombic efficiency for triple-shelled $LiMn_2O_4$ hollow microspheres at a rate of 1 C between 3.5 and 4.3 V.

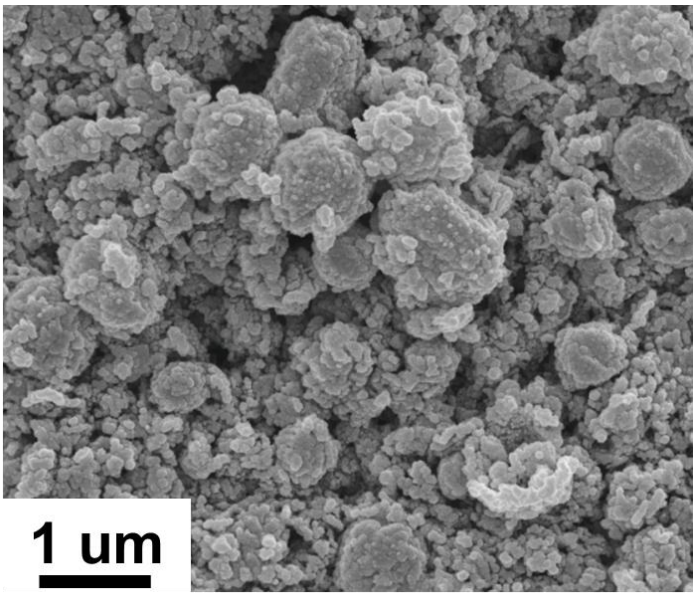

Figure S11 SEM images of the triple-shelled $LiMn_2O_4$ hollow microspheres after 100 cycles.

Table S1 Comparison of the electrochemical performance of $LiMn_2O_4$-based electrode materials in literatures.

$LiMn_2O_4$ materials	Initial discharge capacity (mAh/g) / current density (mA/g)	Capacity fading rate / current density (mA/g) / cycle number	References
$LiMn_2O_4$ nanoparticles	110.9 / 148	0.18% / 148 /100	S2
$LiMn_2O_4$ powder	130 / 148	0.15% / 148 / 50	S3
$LiMn_2O_4$ powder	80.9 / 148		S4
$LiMn_2O_4$ particles	120.4 / 148	0.19% / 148 / 100	S5
$LiMn_2O_4$ particles	114.0 / 148	0.12% / 148 / 100	S6
$LiMn_2O_4$ nanowires	115 / 148	0.15% / 148 / 100	S7
$LiMn_2O_4$ particles	124 / 120	0.18% / 120 / 50	S8
$LiMn_2O_4$/C nanowires	115 / 140	0.87% / 140 / 300	S9
GR/$LiMn_2O_4$ particles	140 / 140	0.1% / 140 / 50	S10
3S-$LiMn_2O_4$-HMSs	115.6 / 148	0.10% / 148 / 200	This work

Table S2 Summary of synthesis conditions of various multi-shelled $LiMn_2O_4$ hollow microspheres.

Structures	Ratio of Li to Mn	Solvent	Adsorption temperature (℃)	Adsorption duration (h)	Calcination temperature (℃)	Heating rate (℃ /min)
Triple-shelled	10:1	H_2O	30	12	600	1
Quadruple-shelled	10:1	H_2O	30	24	600	0.5

Table S3 Summary of parameters of the $LiMn_2O_4$ products according to the nitrogen adsorption–desorption isotherm.

Structures	Specific surface area (m^2/g)	Pore volume (cm^3/g)
Triple-shelled	31.69	0.304
Quadruple-shelled	47.04	0.513

References

[S1] X. Y. Lai, J. Li, B. A. Korgel, Z. H. Dong, Z. M. Li, F. B. Su, J. Du and D. Wang, *Angew. Chem. Int. Ed.*, 2011, **50**, 2738 –2741.

[S2] S. Karaal, H. Kose, A. O. Aydin and H. Akbulut, *Mat. Sci. Semicond. Process.*, 2015, **38**, 397-403.

[S3] B. Hamankiewicz, M. Michalska, M. Krajewski, D. Ziolkowska, L. Lipinska, K. Korona, M. Kaminska and A. Czerwinski, *Solid State Ionics,* 2014, **262**, 9-13.

[S4] T. Y. S. P. Putra, M. Yonemura, S. Torii, T. Ishigaki and T. Kamiyama, *Solid State Ionics*, 2014, **262**, 83-87.

[S5] X. He, J. Wang, H. P. Jia, R. Kloepsch, H. D. Liu, K. Beltrop. and J. Li, *J. Power Sources,* 2015, **293**, 306-311.

[S6] Q. T. Zhang, J. T. Mei, X. M. Wang, W. F. Fan, F. C. Wang, W. J. Lu and F. L. Tang, *J. Alloys Compd.,* 2014, **606**, 249-253.

[S7] D. Y. Kim, P. Muralidharan, H.-W. Lee, R. Ruffo, Y. Yang, C. K. Chan, H. L. Peng, R. A. Huggins and Y. Cui, *Nano Lett.*, 2008, **8**, 3948-3952.

[S8] X. Zhao, M. V. Reddy, H. X. Liu, S. Ramakrishna, G. V. S. Rao and B. V. R. Chowdari, *RSC Advances*, 2012, **2**, 7462–7469.

[S9] W. W. Sun, H. Q. Liu, Y. M. Liu, G. X. Bai, W. Liu, S. S. Guo and X.-Z. Zhao, *Nanoscale*, 2015, **7**, 13173-13180.

[S10] M. H. Pyun and Y. J. Park, *J. Alloys Compd.*, 2015, **643**, S90-S94.